AD-A173 721 THE EMPLOYMENT OF A 3HE-BASED FAST NEUTRON SPECTROMETER TO AUGMENT THE DR..(U) DEFENCE RESEARCH ESTABLISHMENT OTTAWA (ONTARIO) T COUSINS OCT 85 DREO-935 1/1

UNCLASSIFIED F/G 8/4 NL

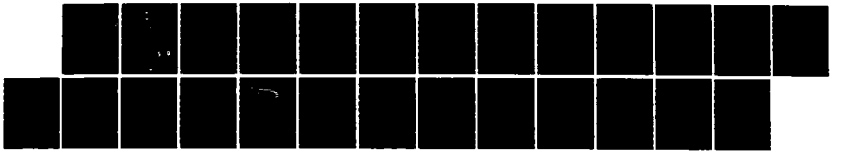

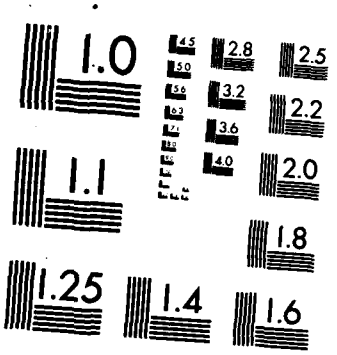

National Defence / Défense nationale

THE EMPLOYMENT OF A ^{3}HE-BASED FAST NEUTRON SPECTROMETER TO AUGMENT THE DREO RADIATION MEASUREMENT SYSTEM

by

T. Cousins

DEFENCE RESEARCH ESTABLISHMENT OTTAWA
REPORT NO. 935

Canada

October 1985
Ottawa

National Defence / Défense nationale

THE EMPLOYMENT OF A ^{3}HE-BASED FAST NEUTRON SPECTROMETER TO AUGMENT THE DREO RADIATION MEASUREMENT SYSTEM

by

T. Cousins
Nuclear Effects Section
Protective Sciences Division

DEFENCE RESEARCH ESTABLISHMENT OTTAWA
REPORT NO. 935

PCN
11A10

October 1985
Ottawa

Abstract

The major radiation spectrometer utilized by DREO for the measurement of both free-field and in-vehicle field has been until recently the NE213 liquid scintillator. In the area of neutron spectroscopy the poor energy resolution and relatively high lower energy threshold are this spectrometer's major drawbacks. With a view to circumventing these problems, DREO recently decided to augment its neutron spectroscopy system with a ^{3}He-based ionization chamber. This report describes the advantages of this detector and outlines the methodology used to generate the energy-dependent response matrix necessary for spectral unfolding. Finally, the unfolded spectra from various radiation sources are presented and compared with theory and other experimental results.

Résumé

Jusqu'à récemment, le principal spectromètre de rayonnement utilisé par le CRDO pour mesurer le rayonnement à l'extérieur et à l'intérieur des véhicules était le détecteur à scintillateur liquide NE213. Les principaux inconvénients de ce spectromètre dans le domaine de la spectroscopie neutroniqe sont sa faible résolution énergétique et son seuil énergétique inférieur relativement élevé. Dans le but de contourner ces problèmes, le CRDO à récemment décidé de muir son système de spectroscopie neutronique d'une chambre d'ionisation à ^{3}He. Le présent rapport décrit les avantages de ce détecteur et donne un apercu des méthodes utilisées pour générer la matrice de réponse en fonction de l'énergie, nécessaire pour traiter les données et ainsi obtenir des spectres. Enfin, on présente les spectres de diverses sources de rayonnement obtenus après traitement des données et on les compare avec ceux prévus par la théorie et avec d'autres résultats expérimentaux.

Introduction

Neutron spectroscopy, as it relates to situations of military importance, has up until now relied almost exclusively on proton-recoil scintillation devices - with the most important of these being the NE213 liquid scintillator. Such spectrometers have the advantage of high detection efficiency, allowing direct measurement of neutron spectra at large, and thus militarily significant distances from high-intensity radioactive sources. At the same time however, scintillators offer relatively poor energy resolution (200 KeV - 500 KeV) and have a lower neutron energy threshold ($E_{th} \simeq 1$ MeV) due to cross-over timing discrimination uncertainties between low energy neutrons and gamma rays. The method chosen to at least partially circumvent these problems at DREO (1) involves the use of BF_3 spectrometers to measure the thermal neutron fluence (below 0.5 eV) and the assumption of a power spectrum of the form $\phi(E) = AE^P$ from 0.5 eV to 0.8 MeV. Such methods are generally reasonable approximations, but do not allow for the existence of any structure in the energy spectrum below 800 KeV. When considering the case of the transmitted spectrum inside an armoured vehicle, however, the existence of "neutron windows" (minima in the neutron cross-section) in steel and other shielding materials would portend much lower energy structure.

Recent developments in the field of high-pressure gas-filled neutron detectors have produced a ^{3}He-based spectrometer which may be of considerable avail in circumventing these aforementioned problems. The FNS-1 fast neutron ionization chamber (SEFORAD-APPLIED RADIATION, EMEK HAYARDEN, ISRAEL) can be shown to have high enough gas pressure (6 atm. ^{3}He) to offer reasonable counting efficiency at low neutron energies, while at the same time affording superb energy resolutions (12 KeV at thermal energies, 25 KeV for 1 MeV neutrons)(2). These features make such a detector attractive for direct air-over-ground measurements of low energy neutron spectra. At higher energies, however, a sharp drop in the ^{3}He (n,p) T cross section (3) renders the spectrometer incapable of producing statistically meaningful results.

This report describes the development and implementation of an energy-dependent response matrix for the ^{3}He spectrometer, enabling unfolding of measured neutron spectra. Two methods of spectral analysis will be discussed. The first embraces a collaborative method with an NE213 spectrometer, whereby the contribution to the low energy spectrum from high energy ($En \geq 3$ MeV) neutrons (as measured by the scintillator) is "stripped off" before unfolding takes place. The second method uses the ^{3}He spectrometer in a "stand alone" mode, where unfolding takes place with no knowledge of the high energy spectral contribution.

Development of Energy-Dependent Response Matrix

Need to Develop Matrix

The measured response of any detector, M(E), to a true spectrum of incident neturons T(E'), may be expressed most conveniently by the convolution integral

$$M(E) = \int_0^\infty R(E,E')T(E')dE' \qquad (1)$$

where R(E,E') is the response function relating to the true energy spectrum at energy E' to the measured spectrum at energy E.

Conversely

$$T(E') = \int_0^\infty R(E',\ E)\ M(E)\ dE \qquad (2)$$

where R(E',E) is meant to represent the inverse of R(E,E').

Since in the field of nuclear data acquisition and analysis, a measured energy spectrum invariably constitutes a discrete or "binned" distribution (as, indeed, is the situation for the unfolded "true" data), it is most suitable to rewrite (2) in matrix form:

$$T_i = \sum_k R_{ik}\ M_k \qquad (3)$$

Here R_{ik} relates the measured counts in bin k to the true counts in bin i. Knowledge of the energy dependent response matrix R_{ik} is essential for accurate deconvolution.

Method of Development

A. Physical Characteristics of the Detector

Understanding of the physical interactions within the ^3He spectrometer required precise knowledge of both its gas filling and physical dimensions. The former would clearly enumerate all possible nuclear reactions to be considered, while the latter defines the active volumes in which these reactions may occur and in which the reaction products may propogate.

The gas composition of the detector, as given by the manufacturer, is:

6 atm	^3He
3 atm	Ar
0.5 atm	CH_4

From this the major possible nuclear reactions are:

1. $^3He(n,p)T$. The large positive Q-value (Q = + 763.8 + .1 KeV (4)) associated with this reaction assures that even thermal (En $\sim$ 0) neutrons will produce pulses with heights well above the noise band (and gamma ray continuum).

2. Elastic scattering with ^3He nuclei. Such reactions produce a flat continuum from E = 0 to E = 3/4 E_n. Clearly this will not interfere with contributions from the $^3He(n,p)T$ reaction unless incident neutrons with energies greater than 4/3 Q ($\gtrsim$ 1 MeV) are present.

3. Proton recoils arising from interactions with methane. Again, a flat distribution of energies from E = 0 to E = E_n will be observed.

4. $^3He(n,d)D$. Owing to the high threshold ($E_{th} \sim 4.5$ MeV) and very small cross section (< 100 mb up to 14 MeV (5)) this reaction was deemed unimportant for low energy neutron spectroscopy, and not considered in the development of the model.

The interplay of the first three reactions in producing a "raw" ^3He spectrum is illustrated in fig (1). Note that here, and in all subsequent plots, the energy scale has been shifted upwards by 764 KeV, resulting in the full energy peak from the (n,p) reaction corresponding to En. The dominance of the peak at En = 0 due to the large thermal cross section of the (n,p) reaction is typical of all ^3He spectra. This peak, while extremely useful for energy calibration, tends on occasion to obscure low energy structure due to pulse pileup effects to be discussed.

The physical dimensions of the FNS-1 ^3He spectrometer are shown in fig (2a). Of particular note is the implementation of a Frisch grid surrounding the annode, to overcome the difficulty of the positional dependence of pulse height common to conventional ion chambers. The volume defined by the two end electrodes, the grid and the cathode may be thought of as the

"active volume" of the detector; any ionization track completely contained in this volume will result in the maximum possible (or "full energy") pulse height being viewed at the anode. Any ionization track extending outside of the volume will result in a smaller pulse height, with the modifications discussed in the next section.

B. Code for Predicting Response Function

A Monte Carlo approach was chosen to predict detector response for neutrons for various incident energies. The procedure for each possible reaction was to allow 30,000 incident monoenergetic neutrons to impinge radially upon the detector, and then to allow the reactions to occur randomly throughout the entire detector volume. The energies, angular distributions and ranges of reaction products were then calculated (6), and their ionizing paths divided into 100 equal segments. Modifications could be made to the observed pulse height due to each event depending on whether these ionization tracks extended outside the active volume. The flow chart in fig (2b) explains this procedure for the (n,p) reaction, with the same principle being applied to the others. Finally the total response of the detector to neutrons of any given energy is simply the cross-section-weighted sums of the calculated responses, i.e.:

$$R_{^3He}(E,E') = \sigma_{n,p}(E)R_{n,p}(E,E') + \sigma_{elas}(E)R_{elas}(E,E') + \sigma_{prot}(E)R_{prot}(E,E')$$

here the suffixes refer to the (n,p) reaction, elastic scattering with ^3He and proton recoil scattering.

Analytical fits were subsequently made to the response functions in order to facilitate a smoothly varying matrix, regardless of bin width. The predicted response functions for neutrons of various energies are shown in fig (3). Note especially the sharp drop off in full energy peak efficiency as neutron energy is increased.

The development of analytical fits to the response function also allowed generation of response matrices of variable upper energy limit. Computer memory requirements have limited useful response matrices to lower-triangular, 100 x 100 blocks (i.e. 5050 non-zero elements stored in a vector array). By varying the upper energy limit, the bin size of the spectrum must also be changed. Ideally, spectra with a bin size of 0.03 MeV or less (upper energy limit of 3 MeV) are desirable, since the bin size is close to the detector resolution. In practice, depending on the hardness of the measured spectrum 5,10 or even 20 MeV upper energy limit matrices are sometimes required - resulting in unfortunate "over-smoothing" of measured spectra due to rebinning before unfolding.

C. Implementation of Response Matrix for Unfolding

The methodology employed for spectral unfolding at DREO (and many other laboratories) was initially developed by Szabo (7) specifically for use with the NE213 scintillator. The unfolding procedure is one of Gaussian elimination whereby all observed counts in the highest energy bin of the spectrum are originally assigned as arising from incident neutrons with that particular corresponding energy. The response vector for that neutron energy is then used to strip off the lower energy contributions from the measured spectrum before proceeding to the next lowest energy bin. The procedure is then repeated to span the entire measured spectrum.

Such a procedure relies a priori upon the fact that observed counts in the top bin are due to neutrons of the corresponding energy - i.e. a strong "full energy" efficiency is necessary for reliable unfolding. As seen for the case of ^{3}He spectrometry, the rapidly falling ^{3}He(n,p)T above En $\sim$ 3 MeV may render this assumption inappropriate. Thus, depending on the hardness of the incident neutron energy spectrum, the unfolding code may have to be modified as below:

Consider again equation (1)

$$M(E) = \int_0^\infty R(E,E')\ T(E')dE'$$

Convenient subdivision yields

$$M(E) = \int_0^{E_c} R(E,E')T(E')dE' + \int_{E_c}^\infty R(E,E')T(E')dE'$$

where E_c is some arbitrary cut-off energy, usually, for the purpose of the experiments to be discussed here, approximately 3 MeV.

The second term on the right hand side of the equation may be evaluated directly so long as T(E') is known. It will be shown that T(E') may come from either the coincident measurements of another detector (NE213) or from theory.

Then, rewriting,

$$M(E) = \int_{\circ}^{E_C} R(E,E')\ T_{<}(E')dE' + \int_{E_C}^{\infty} R(E,E')\ T_{>}(E')\ dE'$$

$$= \int_{\circ}^{E_C} R(E,E')\ T_{<}(E')dE' + C(E)$$

so where $T_<$ and $T_>$ represent the fraction of the true spectra below and above E_C respectively and $C(E)$ is the high energy contribution to $M(E)$.

$$M_S(E) = M(E) - C(E) = \int_{\circ}^{E_C} R(E,E')\ T_{<}(E')dE'$$

where $M_S(E)$ is that portion of the measured spectrum due to neutrons below E_C.

Once $M_S(E)$ has been evaluated, unfolding may proceed since now it is assured that all measured counts $M_S(E)$ correspond to neutrons of energy $< Ec$.

It should be noted in passing that for a soft neutron spectrum, the subtraction procedure may not be necessary, i.e. if the low energy contribution from all neutrons with energies above E_C is statistically small, then the assumption $C(E) \sim 0$ may be valid, and unfolding may proceed directly - this will be referred to as the "stand alone" method.

Experimental

1. Full Energy Peak Analysis

The full-energy-peak efficiency (equivalent to the "photopeak" in gamma-ray spectroscopy) may be calculated simply from the $R_{n,p}$ matrix as

Absolute Peak Efficiency

$$= \varepsilon(E) = (N)\ (5.09 \times 10^{-4})\sigma_{n,p}(\text{barns})(E)$$

where N is the number (of out of 30,000) of (n,p) interactions resulting in full energy deposition. This parameter is of significance since it is

elementary to measure directly - there being no unfolding needed - and thus offers quick verification of the Monte Carlo method. The full energy peak efficiency is also a desirable quantity to know when using the ^{3}He spectrometer to monitor monoenergetic neutron production from a particle accelerator (this procedure has found great use at DREO). Again simply dividing by the full energy peak efficiency gives the incident neutron fluence - negating the need for extensive computer analysis. Toward these ends the ^{3}He ionization chamber was exposed to monoenergetic neutrons, produced by the DREO Van de Graaff particle accelerator, which spanned the energy range 0.2-6.0 MeV. During each run the fluence was also calculated from knowledge of target thickness and beam current, measured by a calibrated long counter, and, for energies in excess of 1 MeV, measured by a calibrated NE213 spectrometer. The results of these experiments are plotted in fig (4). Also plotted is the normalized $^{3}He(n,P)T$ cross section, which demonstrates the effects of wall and end effects as a function of increasing neutron energy. The agreement between theory and experiment is in general quite good. These results may be compared directly to the work of Sailor and Prussin (8) and Franz (9). Unfortunately these experimenters presented only graphical results, but agreement appears reasonable.

2. Demonstrating Full Energy Response Validity for Monoenergetic Neutrons

The analysis of the measured monoenergetic neutron spectra is compared with the prediction of the unfolding code in fig (5). Here the raw measured spectrum is shown in relation to the spectrum obtained by folding a monoenergetic neutron fluence (determined as above) with the calculated response matrix. Fig. 6 shows the unfolded spectra from the raw data.

3. Experiments with ^{252}Cf

As an examination of the reliability of the unfolding technique the detector was exposed to a fission spectrum from the calibrated ^{252}Cf source at Royal Military College, Kingston. The spectral shape is defined by the well-known Watt function as:

$$\Phi(E) = 0.373\ N \exp(-0.88E) \sinh(\sqrt{2E})$$

where N = source strength (n/sec)

The strength of this particular source has been measured by the National Bureau of Standards, and was 7.7×10^7 n/ sec on the day of the experiments. The unfolded spectra measured 50 cm from the source are shown in figs 7 (a),(b) and (c) due to unfolding with matrices having upper energy limits of 3,5 and 10 MeV respectively, and are compared with the theoretical Watt spectrum. Note the good agreement resulting from unfolding with the two lower energy matrices, while unfolding with the 10 MeV matrix is unreliable due to statistical variations combined with small full energy peak efficiency. Note that above $E_n \sim 2$ MeV, the 3 MeV matrix unfolding shows significant variation due to higher-energy contribution. Unfolding with the 5 MeV matrix reveals little higher-energy contribution due to the nature of the spectrum. Both spectra show a significant low energy component due to room return.

The 10 MeV matrix unfolded spectrum was reanalyzed by first subtracting the high energy contribution due to neutrons with energies in excess of 5 MeV (as determined by the Watt spectrum) and then performing the unfolding. The results are shown in Fig 8 and reveal good agreement with theory.

4. Experiments at Aberdeen Proving Ground

Measurements for neutron spectra at various distances from the bare unshielded core of the Aberdeen Pulsed Radiation Facility, Aberdeen, Maryland using a NE213 spectrometer have been previously reported (1). Experiments were performed again with the ^{3}He spectrometer and the NE213 spectrometer at the same distance from the core, with the complete results to be presented elsewhere. The results shown in fig (9) are for the measured spectrum at 1.087 km from the core. The figure compares the neutron fluences determined from the ^{3}He unfolding (using a 3 MeV matrix) the NE213 unfolding and theoretical calculations (10). All three sets of results are in excellent agreement.

5. Extension to Higher Energy Neutrons

With the development of enhanced radiation weapons, the measurement of higher energy neutron fluences has become important militarily. While it can be anticipated that the ^{3}He spectrometer will be of limited use for such direct measurements, all enhanced radiation weapon exhibit a significant low energy component, which becomes more predominant as range from the weapon is increased. Thus a knowledge of the performance of the ^{3}He spectrometer in such a neutron environment is important.

Toward this end an experiment was conducted in which accelerator produced 16.7 MeV neutrons were allowed to impinge upon a depleted ^{235}U sphere. The resultant neutron spectrum offers reasonable similarity with that produced by an enhanced radiation weapon, in the sense that it has both fission and fusion components. In the experiments both the ^{3}He and NE213 spectrometers were located at the same distance (1m) and angle (30°) with respect to the beam target. Since the small ^{3}He detector efficiency resulted in no statistically meaningful full energy counts, unfolding was impossible without first stripping off the high energy component. The cutoff energy, Ec, was chosen to be 3 MeV, with the NE213 measured spectrum being used to give the higher energy component. The subsequent low energy unfolded spectrum is shown in fig (10) compared to the unfolded NE213 spectrum. The good agreement bodes well for a benevolent symbiotic relationship between the two detectors, regardless of the incident neutron energy spectrum.

Associated Problems

1. Spurious Background Structure

A typical background spectrum acquired with the ^{3}He detector (acquisition time = 250,000 sec) is shown in fig (11). The spectrum is dominated by the strong thermal ($E_n \sim 0$) neutron peak, as expected, due to high detector efficiency. In addition, however, one should note the manifestation of three broad peaks centred roughly at 3, 4.5 and 6.5 MeV respectively. Proposed origins for these peaks range from cosmic ray interactions to electronic sparking effects; however no satisfactory explanation exists. The peaks are always present, independent of detector location or orientation. The low rate at which these peaks accumulate, however, make their existence troublesome only when very soft low intensity measurements are being considered - as, for example, was the case for the measurements at 1 km from the reactor core at Aberdeen Proving Ground. A simple spectral subtraction procedure suffices to eliminate these effects, with the only drawback being an attendant loss of statistical precision.

2. Pulse Pileup Effects

The dominance of the thermal peak in all measured spectra combined with the long (2-6 μ sec) shaping times required on the spectroscopy amplifier (to accommodate pulses from the preamp) results in pileup effects due to summing creating a spurious peak with neutron energy 0.76 MeV. This peak is evident in all spectra in which there is a significant counting rate, and the effect is demonstrated pictorially in fig (12), which represents the raw data measured 100 m from the ARPF core.

One suggested mechanism for removal of pileup effects has been given by Evans (11). It involves a mathematical model of the pileup which is arbitrarily scaled in order to "just remove" the thermal peak contribution. Implementation of this method on our measured spectra proved unsatisfactory due to gain non-linearity and low energy gamma-ray effects. The method chosen here was simply choosing by eye the pileup area and performing a semi-logarithmic fit connecting the data channels on each side of this area, since most spectra approximated this form. Both methods unfortunately result in a smoothed spectrum, which may tend to mask any structure present around the pileup region. For optimum performance then, the detector should be operated in an environment in which the thermal detection rate is low enough to negate pileup effects, but in which the total counting rate is high enough to overwhelm the spurious background effects. In some cases, it may indeed be necessary to divide the experimental run into two segments, one at high power to overide background high energy contributions, and the other at low power to guard against low energy pileup.

Conclusions

The usefulnes of a ^{3}He fast neutron ionization chamber has been clearly demonstrated in spectroscopy for situations of military importance. The detector can be used in a "stand-alone" mode for soft spectral measurements (eg fission sources) up to approximately 5 MeV. For harder sources (eg fusion) a (NE213) measured or theoretically generated spectrum must be used to first strip off high energy neutron contributions. The ^{3}He spectrometer will be useful in providing information to fill the gaps in previously measured spectra.

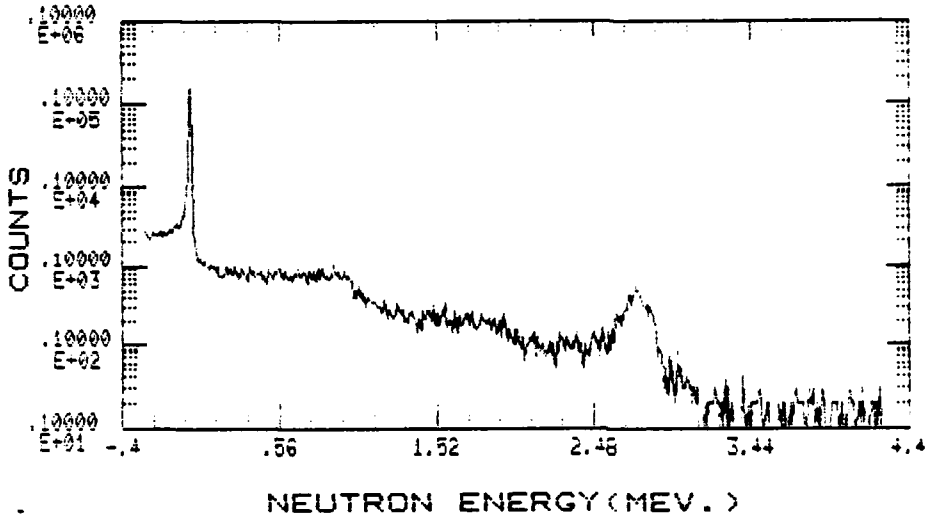

Figure 1: Measured raw ^{3}He spectrum from monoenergetic 2.7 MeV neutrons. The three main reactions components are indicated. Note also the dominance of the thermal (En $\sim$ 0) peak.

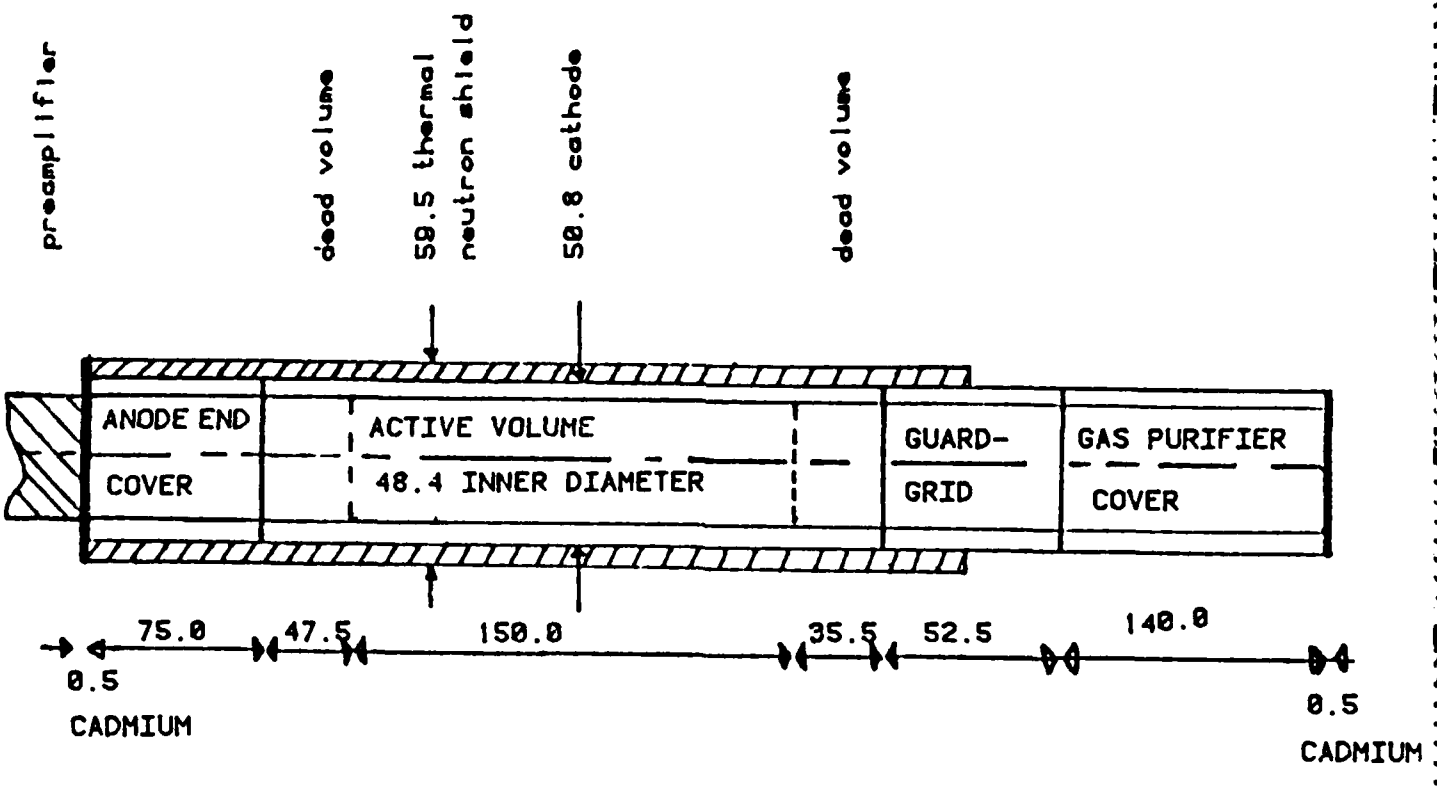

Figure 2(a): Physical dimensions of the FNS-1 spectrometer used in Monte Carlo code

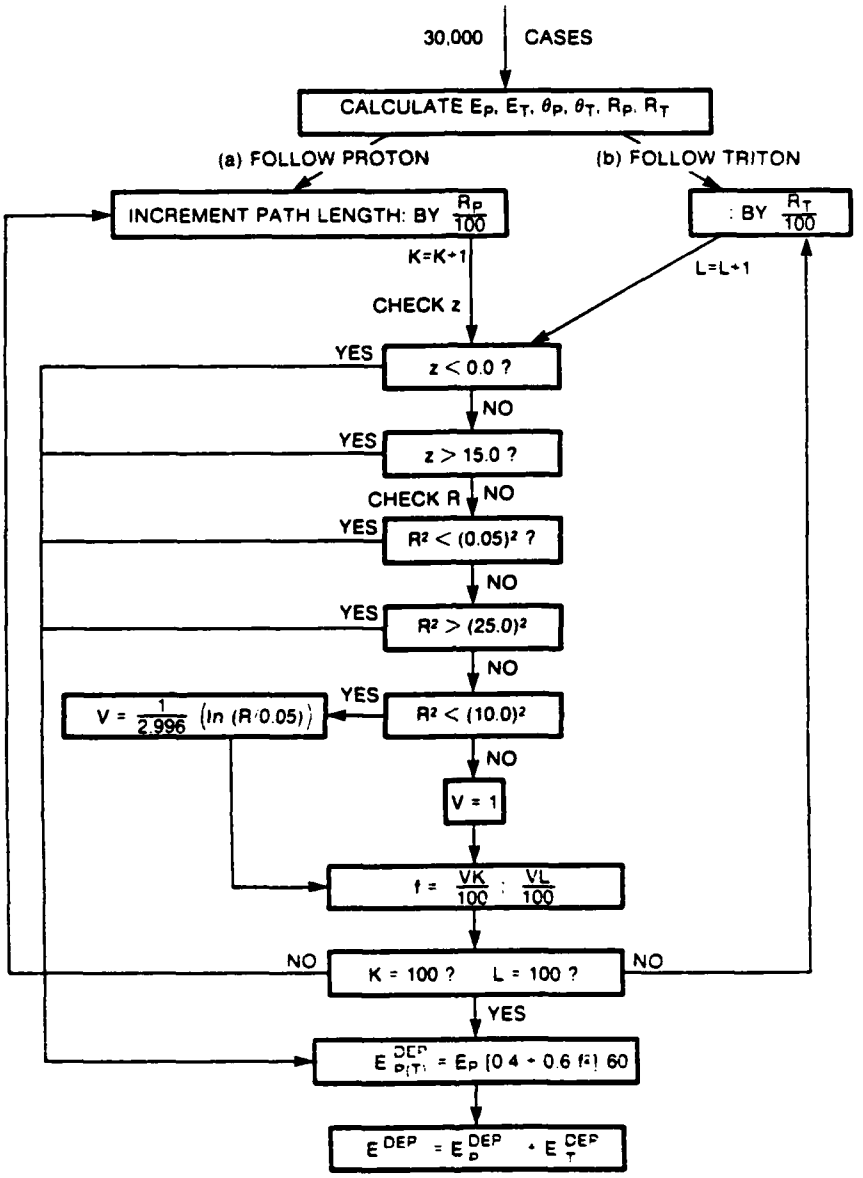

Figure 2(b): Flow chart illustrating Monte Carlo techniques applied to determine ^{3}He energetic response function.

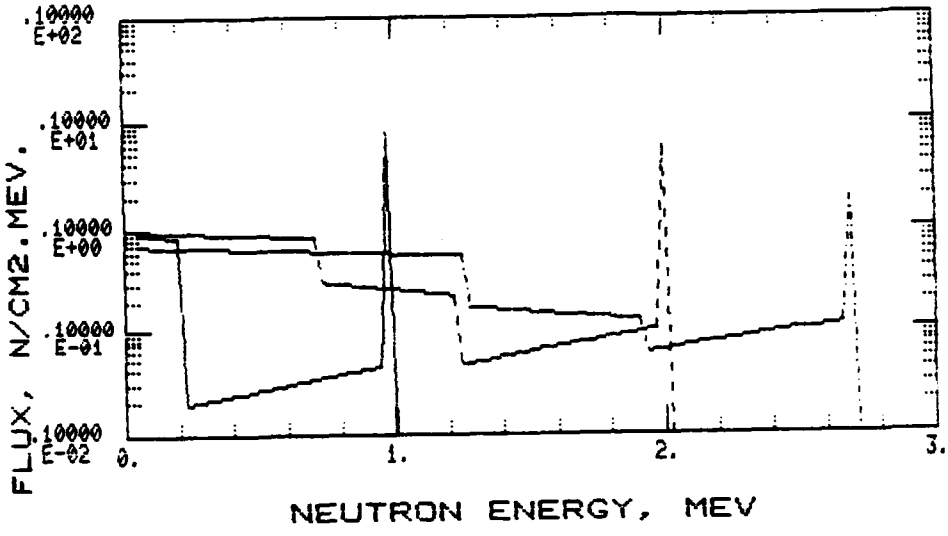

Figure 3: Predicted ^{3}He response function to incident monoenergetic neutrons of 1.0, 2.0 and 2.7 MeV.

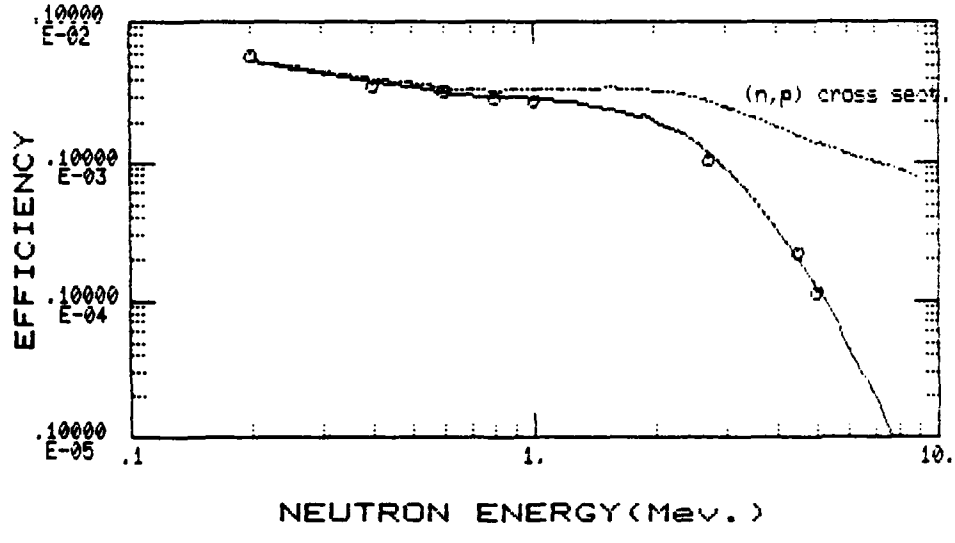

Figure 4: Experimental (circles) and theoretical (solid line) full energy peak efficiencies of the ^{3}He spectrometer. The normalized (n,p) cross section is plotted to show the increasing importance of wall and end effects as neutron energy is increased.

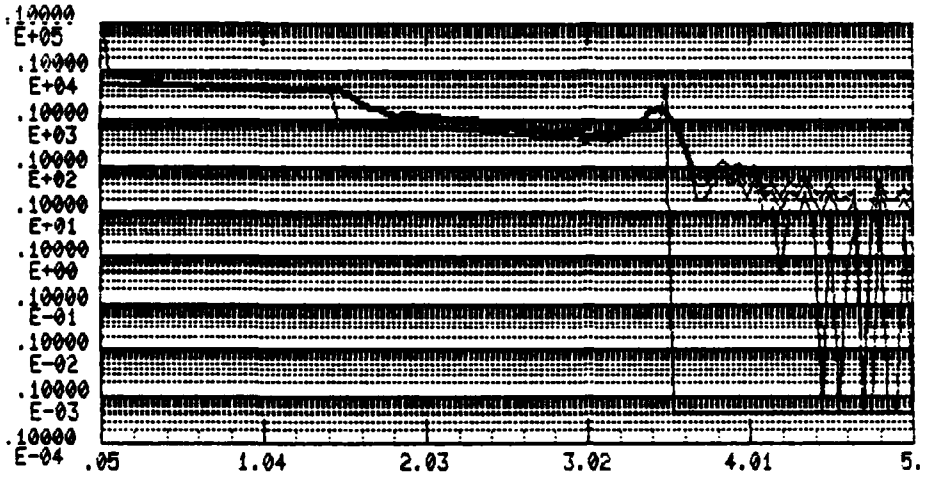

Figure 5: Measured ^{3}He spectrum from monoenergetic 3.5 MeV n's, compared with incident spectrum of 3.5 MeV n's (flux determined by NE213 measurement) folded with response matrix. The effect of resolution (caused by accelerator target thickness) is evident both on the peak and recoil edge.

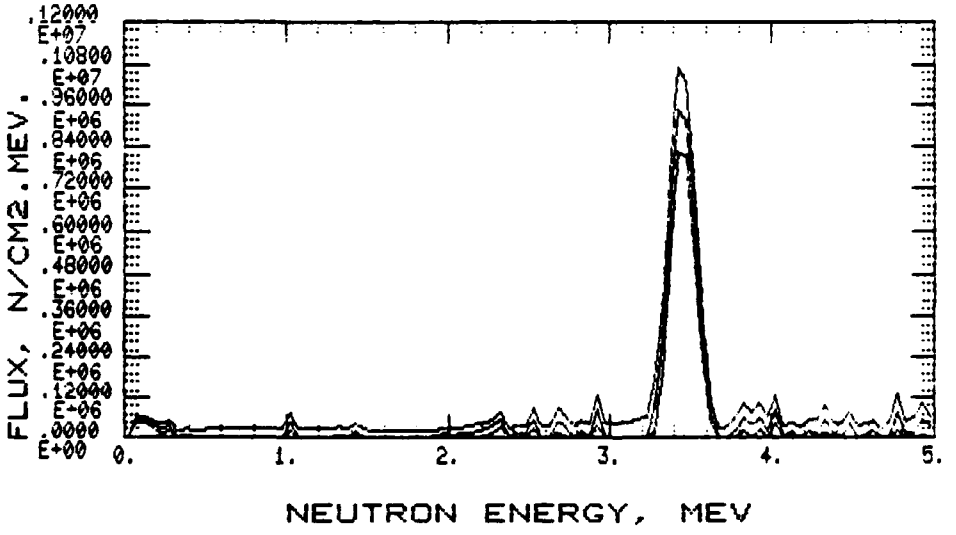

Figure 6: Unfolded spectrum (with errors) from raw data in Figure 5.

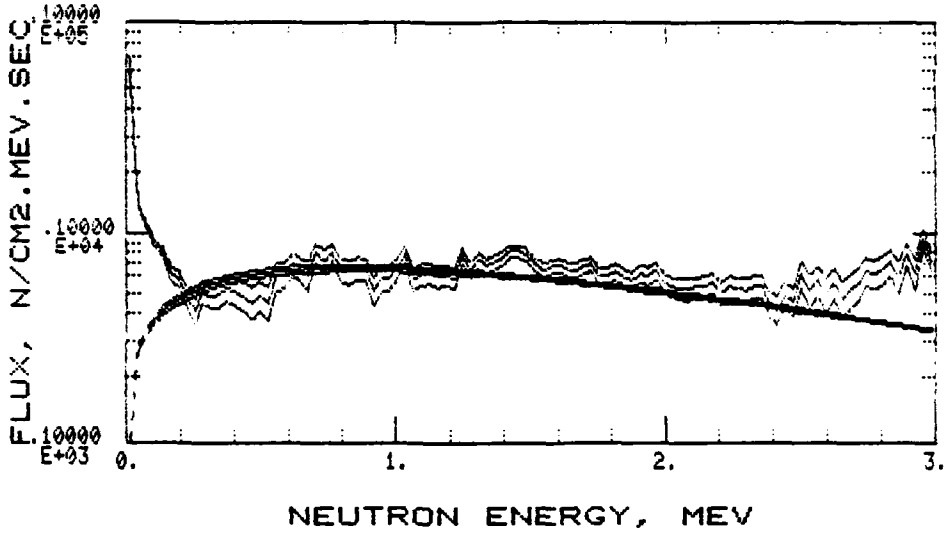

Figure 7(a): Unfolded ^{3}He spectrum (solid line), with, errors, from ^{252}Cf irradiation compare with theoretical Watt spectrum (broken line) following unfolding with 3 MeV response matrix.

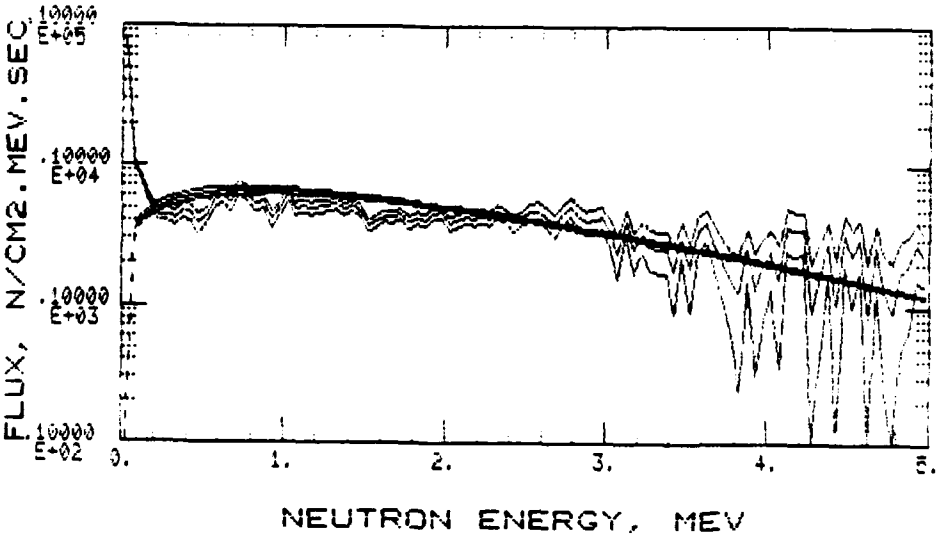

Figure 7(b): Unfolded ^{3}He spectrum (solid line), with errors, from ^{252}Cf irradiation compared with theoretical Watt spectrum (broken line) following unfolding with 5 MeV response matrix.

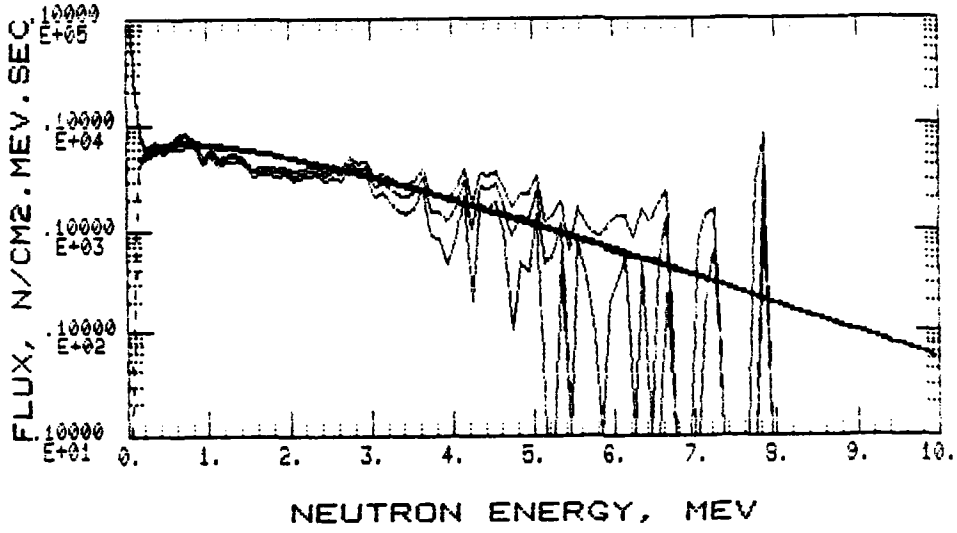

Figure 7(c): Unfolded ^{3}He spectrum (solid line), with errors, from ^{252}Cf irradiation compared with theoretical Watt spectrum (broken line) following unfolding with 10 MeV response matrix.

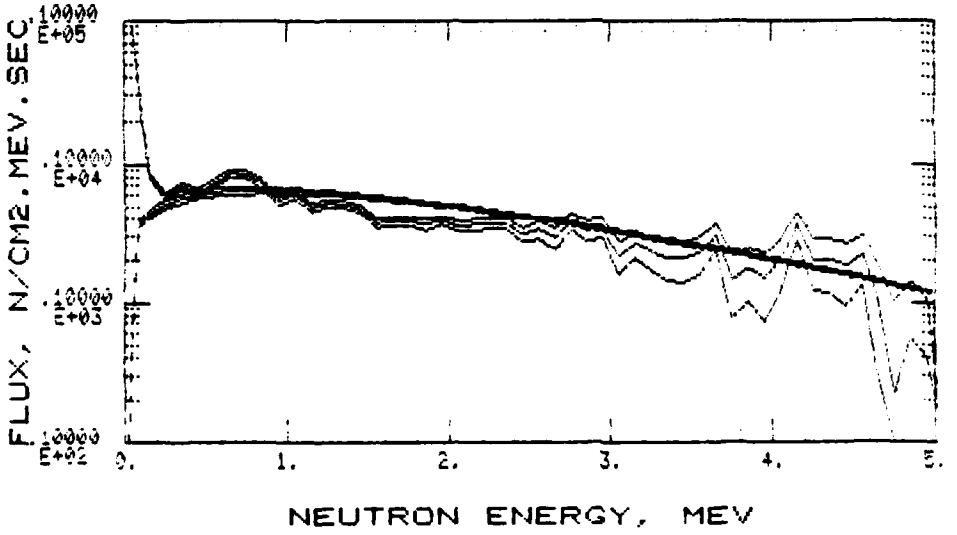

Figure 8: Unfolded ^{3}He spectrum (solid line), with errors, from ^{252}Cf irradiation compared with the theoretical Watt spectrum (broken line). The high energy contributions (above 5 MeV were first stripped off, and then unfolding with the 10 MeV response matrix took place.

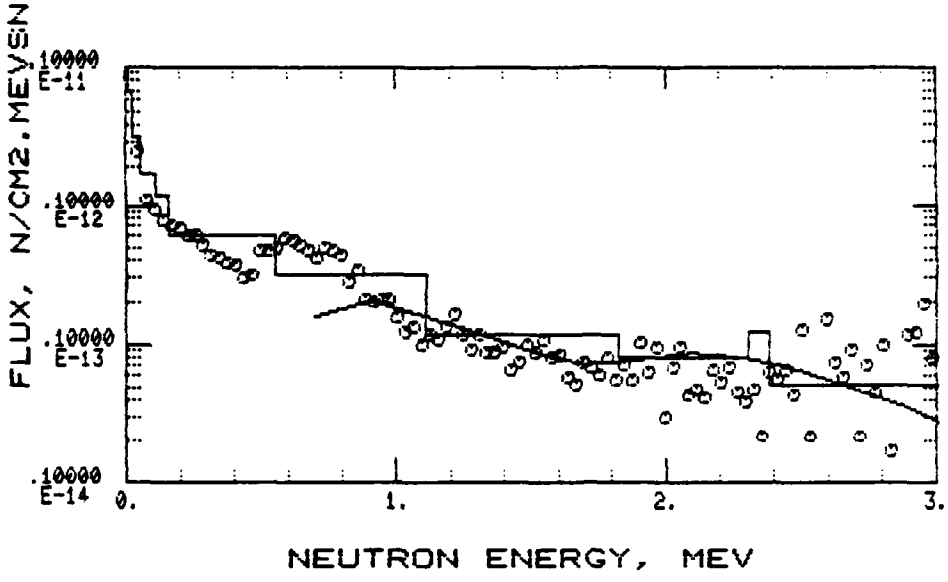

Figure 9: Comparison of measured ^{3}He (circles) and NE213 (smooth line), spectra with theoretical prediction of neutron spectrum at 1 km from the APG core.

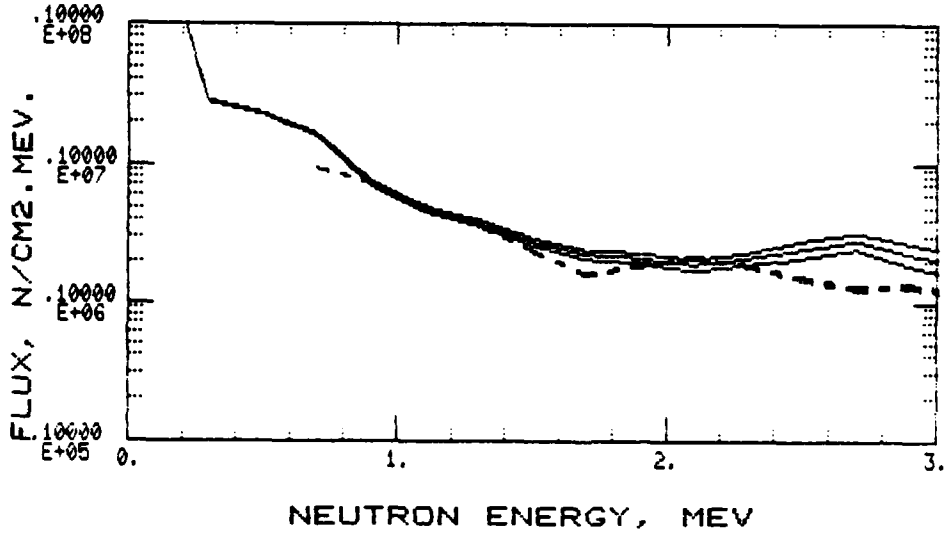

Figure 10: Comparison of measured ^{3}He (solid line) spectrum with errors with measured NE213 (broken line) spectrum for mixed fission/fusion source as described in the text.

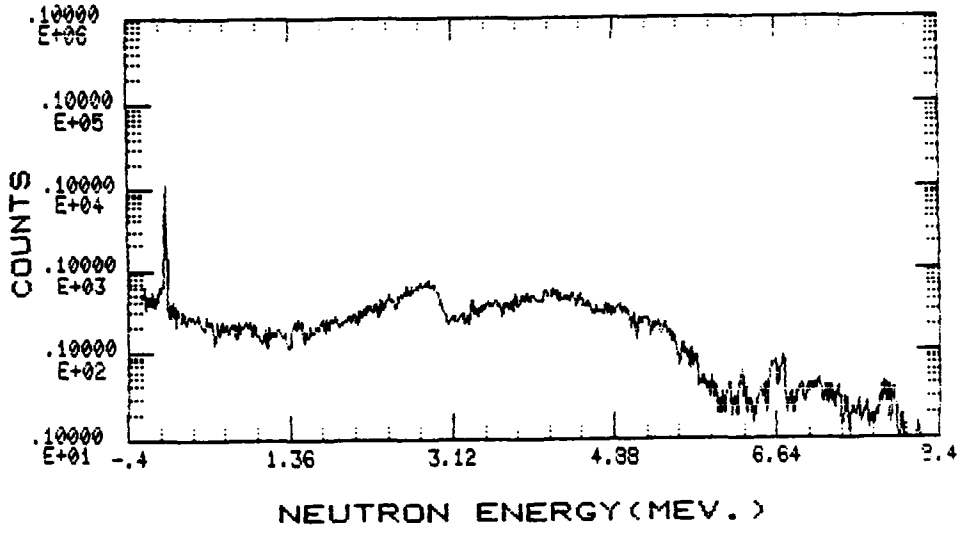

Figure 11: ^{3}He Background Spectrum. Note the manifestation of anomalous structure at high energies, which may tend to obscure real events if the counting rate is low enough.

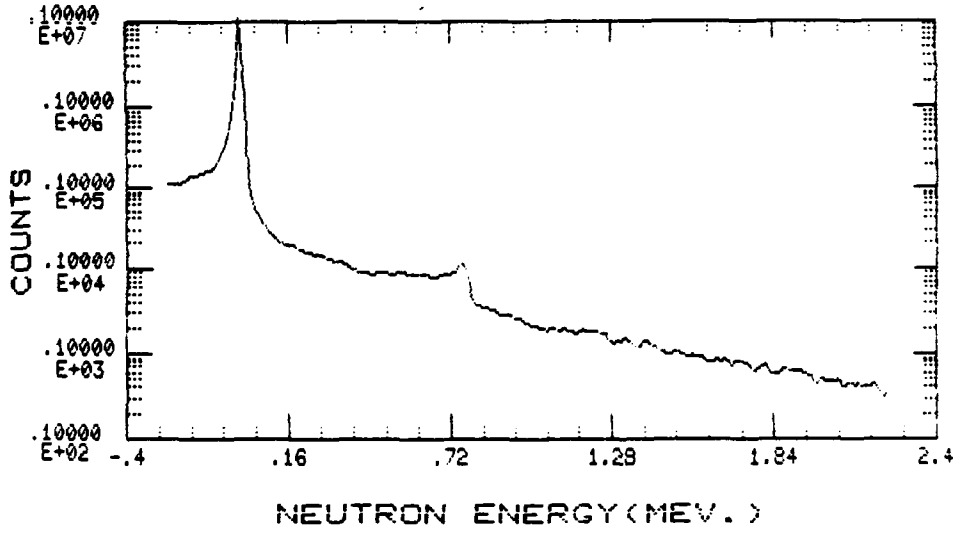

Figure 12: Raw ^{3}He data measured 100 m from APRF core. Note the pileup peak at E_n = 0.76 MeV which must be removed before unfolding takes place.

References

1. H.A. Robitaille and B.E. Hoffarth, DREO Report No. 835, December 1980, Department of National Defence, Canada.

2. J.M. Cuttler, Ph.D. Thesis, Technion, Israel (1971).

3. BNL 325, Third Edition, Vol 1, June 1973.

4. A.H. Wapstra and K. Bos, At. Data and Nucl. Data Tables 20 (1970).

5. J.N. Bradbury and L. Stewart, Bull. Am. Phys. Soc., 3, 417 (1958).

6. J. Flugge, Corpuscles and Radiation in Matter II, 1958, Springer Verlag, 211.

7. F.P. Szabo, DREO Report No. 637, July 1971, DND, Canada.

8. W.C. Sailor and S.G. Prussin, NIM, 173, 511 (1980).

9. H. Franz et al., NIM, 144, 253 (1977)

10. D. Kaul, Science Applications Incorporated, Private Communication

11. A.A. Evans, E.F. Bennett and T.J. Yule, Proceedings of Health Physics Meeting, New Orleans, June 5, 1984.

AD-A173 721

UNCLASSIFIED

Security Classification

DOCUMENT CONTROL DATA - R & D

(Security classification of title, body of abstract and indexing annotation must be entered when the overall document is classified)

1. ORIGINATING ACTIVITY Defence Research Establishment Ottawa	2a. DOCUMENT SECURITY CLASSIFICATION Unclassified 2b GROUP

3. DOCUMENT TITLE

The Employment of a ^{3}He-Based Fast Neutron Spectrometer to Augment the DREO Radiation Measurement System

4. *DESCRIPTIVE NOTES (Type of report and inclusive dates)*

DREO Report

5. AUTHOR(S) (Last name, first name, middle initial)

Cousins, T.

6. DOCUMENT DATE October 1985	7a. TOTAL NO OF PAGES	7b NO OF REFS 11
8a. PROJECT OR GRANT NO. 11A20	9a. ORIGINATOR'S DOCUMENT NUMBER(S)	
8b. CONTRACT NO.	9b. OTHER DOCUMENT NO.(S) (Any other numbers that may be assigned this document)	

10. DISTRIBUTION STATEMENT

UNLIMITED

11 SUPPLEMENTARY NOTES	12. SPONSORING ACTIVITY DREO

13 ABSTRACT

The major radiation spectrometer utilized by DREO for the measurement of both free-field and in-vehicle field has been until recently the NE213 liquid scintillator. In the area of neutron spectroscopy the poor energy resolution and relatively high lower energy threshold are this spectrometer's major drawbacks. With a view to circumventing these problems, DREO recently decided to augment its neutron spectroscopy system with a ^{3}He-based ionization chamber. This report describes the advantages of this detector and outlines the methodology used to generate the energy-dependent response matrix necessary for spectral unfolding. Finally, the unfolded spectra from various radiation sources are presented and compared with theory and other experimental results.

DSIS

UNCLASSIFIED
Security Classification

KEY WORDS

^{3}He
NE213
Radiation Spectroscopy
Neutron
Core
Fission
Fusion

INSTRUCTIONS

1. ORIGINATING ACTIVITY: Enter the name and address of the organization issuing the document.

2a. DOCUMENT SECURITY CLASSIFICATION: Enter the overall security classification of the document including special warning terms whenever applicable.

2b. GROUP: Enter security reclassification group number. The three groups are defined in Appendix 'M' of the DRB Security Regulations.

3. DOCUMENT TITLE: Enter the complete document title in all capital letters. Titles in all cases should be unclassified. If a sufficiently descriptive title cannot be selected without classification, show title classification with the usual one-capital-letter abbreviation in parentheses immediately following the title.

4. DESCRIPTIVE NOTES: Enter the category of document, e.g. technical report, technical note or technical letter. If appropriate, enter the type of document, e.g. interim, progress, summary, annual or final. Give the inclusive dates when a specific reporting period is covered.

5. AUTHOR(S): Enter the name(s) of author(s) as shown on or in the document. Enter last name, first name, middle initial. If military, show rank. The name of the principal author is an absolute minimum requirement.

6. DOCUMENT DATE: Enter the date (month, year) of Establishment approval for publication of the document.

7a. TOTAL NUMBER OF PAGES: The total page count should follow normal pagination procedures, i.e., enter the number of pages containing information.

7b. NUMBER OF REFERENCES: Enter the total number of references cited in the document.

8a. PROJECT OR GRANT NUMBER: If appropriate, enter the applicable research and development project or grant number under which the document was written.

8b. CONTRACT NUMBER: If appropriate, enter the applicable number under which the document was written.

9a. ORIGINATOR'S DOCUMENT NUMBER(S): Enter the official document number by which the document will be identified and controlled by the originating activity. This number must be unique to this document.

9b. OTHER DOCUMENT NUMBER(S): If the document has been assigned any other document numbers (either by the originator or by the sponsor), also enter this number(s).

10. DISTRIBUTION STATEMENT: Enter any limitations on further dissemination of the document, other than those imposed by security classification, using standard statements such as

(1) "Qualified requesters may obtain copies of this document from their defence documentation center."

(2) "Announcement and dissemination of this document is not authorized without prior approval from originating activity."

11. SUPPLEMENTARY NOTES: Use for additional explanatory notes.

12. SPONSORING ACTIVITY: Enter the name of the departmental project office or laboratory sponsoring the research and development. Include address.

13. ABSTRACT: Enter an abstract giving a brief and factual summary of the document, even though it may also appear elsewhere in the body of the document itself. It is highly desirable that the abstract of classified documents be unclassified. Each paragraph of the abstract shall end with an indication of the security classification of the information in the paragraph (unless the document itself is unclassified) represented as (TS), (S), (C), (R), or (U).

The length of the abstract should be limited to 20 single-spaced standard typewritten lines, 7½ inches long.

14. KEY WORDS: Key words are technically meaningful terms or short phrases that characterize a document and could be helpful in cataloging the document. Key words should be selected so that no security classification is required. Identifiers, such as equipment model designation, trade name, military project code name, geographic location, may be used as key words but will be followed by an indication of technical context.

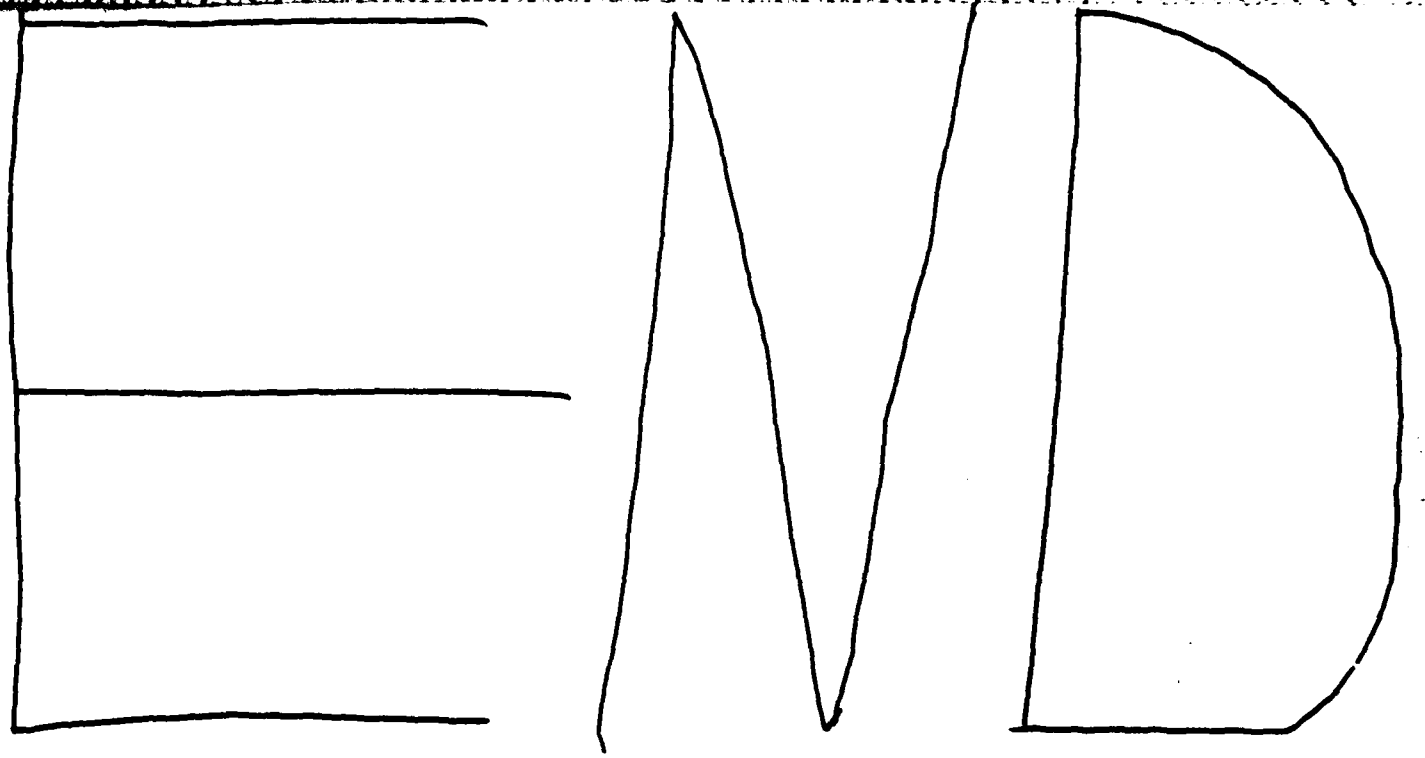

12-86

DTIC